

# Making thermal rate constant calculations reliable using best practices: case study of $\text{OH} + \text{HBr} \rightarrow \text{Br} + \text{H}_2\text{O}$

Ivan S. Novikov,<sup>1, a)</sup> Edgar M. Makarov,<sup>1, b)</sup> Alexander V. Shapeev,<sup>1, c)</sup> and Yury V. Suleimanov<sup>2, d)</sup>

<sup>1)</sup>*Skolkovo Institute of Science and Technology, Skolkovo Innovation Center, Nobel St. 3, Moscow 143026, Russia*

<sup>2)</sup>*Computation-based Science and Technology Research Center, The Cyprus Institute, 20 Konstantinou Kavafi Street, Nicosia 2121, Cyprus<sup>e)</sup>*

(Dated: 6 June 2022)

In the present work we apply the combination of Moment Tensor Potential (MTP) and Ring Polymer Molecular Dynamics (RPMD) to the calculation of the thermal rate constants of the  $\text{OH} + \text{HBr} \rightarrow \text{Br} + \text{H}_2\text{O}$  chemical reaction at different temperatures. The MTP was parameterized using the active learning (AL) algorithm to the data obtained with the spin-unlimited method of explicitly correlated coupled clusters with allowance for double and partial allowance for triple excitations (UCCSD(T)-F12a). The considered elementary reaction represents a significant challenge for dynamics simulations due to a light atom transfer along a non-trivial reaction energy path. We compare thus obtained RPMD-AL-MTP rate constants with the ones obtained previously using the quasi-classical trajectories (QCT) and the POTLIB potential energy surface (PES) as well as with the experimental rate constants. We demonstrate that the RPMD rate constants are systematically closer to the experimental rate constants than the QCT ones. We conclude that the proposed methodology based on combining the best practices for electronic structure calculations, PES construction and dynamic simulations makes theoretical estimation of thermal rate constants reliable and can be with certainty extended to more complex chemical reactions in future.

## I. INTRODUCTION

Machine-learning interatomic potentials (MLIPs) are gradually becoming a popular practical choice for molecular simulations in physics, chemistry, and materials science. One of such widely used functional forms of MLIPs is the Moment Tensor Potential (MTP) which was proposed in 2016 for single-component materials<sup>61</sup> and later, in 2018, generalized to the case of multi-component materials<sup>25</sup>, and applied to solving many problems of condensed-phase atomistic simulation<sup>19,21,23,24,31,35,37,38,41–44,50,55,57,68</sup>. In addition, a fully automated method was proposed for on-the-fly construction of potential energy surfaces (PESs) during the calculations of thermal rate constants of gas-phase chemical reactions. The method is based on combining (1) one of the most reliable full-dimensional methods for calculating thermal rate constants, Ring Polymer Molecular Dynamics (RPMD<sup>6,10,11,63</sup>), that was implemented in the RPMDrate code<sup>66</sup> and successfully applied to many prototypical gas-phase chemical reactions<sup>2,4,7,14,16,17,20,26–29,36,39,40,51–54,58,63–65</sup>, and (2) the active learning (AL)<sup>22,56</sup> of MTP (AL-MTP) algorithm implemented in the MLIP-2 code<sup>47</sup>. So far, the combination of RPMD and AL-MTP methods was successfully validated during model rate calculations for two representative thermally activated chemical reactions, namely,  $\text{OH} + \text{H}_2 \rightarrow \text{H} + \text{H}_2\text{O}$ <sup>46</sup> and  $\text{CH}_4 + \text{CN} \rightarrow \text{CH}_3 + \text{HCN}$ <sup>46</sup>, and one prototypical bar-

rierless chemical reaction  $\text{S} + \text{H}_2 \rightarrow \text{SH} + \text{H}^{49}$  in which AL was parameterized to the data from previously generated analytical PESs.

It is worth noting that, before the development of MLIPs, several methods for construction of analytical PESs were proposed and the corresponding libraries were implemented. Such PESs were mainly based on the fitting of polynomials to *ab initio* data. In 2002, a modified Shepard interpolation<sup>18</sup> of PESs was successfully applied to various chemical reactions. This approach is implemented in the Grow package<sup>9</sup>. In 2009, the permutationally invariant PESs in Morse-type variables of all the internuclear distances were proposed. The accuracy of these PESs were verified for such systems as  $\text{CH}_5^+$ ,  $(\text{H}_2\text{O})_2$ , and  $\text{CH}_3\text{CHO}$ <sup>5</sup>. Since 2001, PESs created by various researchers for a variety of chemical systems have been collected in the POTLIB package as a consistent set of computer codes. The package contains PESs for a number of triatomic and polyatomic chemical systems<sup>15</sup>. The number of PESs in POTLIB library keeps growing nowadays; in particular, in 2014 a permutationally invariant PES<sup>5</sup> for the  $\text{OH} + \text{HBr} \rightarrow \text{Br} + \text{H}_2\text{O}$  reaction was constructed and added to POTLIB. Quasiclassical trajectories (QCT) were used to calculate this chemical reaction rate over the temperature range of 5–500 K<sup>12,13</sup>.

Let us take a closer look at the last example. The  $\text{OH} + \text{HBr} \rightarrow \text{Br} + \text{H}_2\text{O}$  reaction represents a significant challenge for dynamics simulations due to the quantum effects of nuclear motions during a light atom (hydrogen) transfer along a rather non-trivial reaction energy path with both an energy barrier and a pre-barrier complex formation region (see Section III A). This reaction is of great importance for stratospheric chemistry as it is the major process by which atomic bromine, an active ozone depletion catalyst, is regenerated from the relatively stable hydrogen bromide<sup>70</sup>. This reaction is also important in combustion chemistry where it has been

<sup>a)</sup>Electronic mail: i.novikov@skoltech.ru

<sup>b)</sup>Electronic mail: Edgar.Makarov@skoltech.ru

<sup>c)</sup>Electronic mail: a.shapeev@skoltech.ru

<sup>d)</sup>Electronic mail: yury.suleymanov@gmail.com

<sup>e)</sup>Present address: American Association for the Advancement of Science, 1200 New York Ave NW, Washington, DC 20005

shown to contribute to the mechanism by which some brominated compounds act as fire retardants<sup>8</sup>. Therefore, this system is not only interesting from the point of view of validating theoretical approaches for calculating the rate constants, but also has practical importance.

In this paper we extend the combination of RPMD and AL-MTP to the problem of direct parametrization to *ab initio* data and use this combination for predicting the OH + HBr  $\rightarrow$  Br + H<sub>2</sub>O reaction rate constants at different temperatures. More specifically, we calculate the RPMD rate constants using (1) the POTLIB PES, (2) the MTP fitted to the POTLIB PES energies, and, finally, (3) the MTP fitted to quantum-mechanical energies. We compare these rate constants with the ones previously calculated with the QCT method using the POTLIB PES<sup>13</sup>, and with the experimental rate constants.

This paper is organized as follows. In Section 2, we describe the AL-MTP methodology for automated construction of PES. In Section 3, we present and discuss the results of rate constants calculations. Finally, in Section 4 we make the conclusions regarding our comparative analysis of RPMD/MTP and QCT/POTLIB methodologies for calculating rate constants.

## II. METHODOLOGY

### A. Moment Tensor Potentials

MTP is a local potential in the sense that the energy of a configuration  $\mathbf{x}$  is partitioned into a sum of contributions of each of  $N$  atoms

$$E^{\text{MTP}} = \sum_{i=1}^N V_i = \sum_{i=1}^N \sum_{\alpha} \xi_{\alpha} B_{\alpha}(r_i), \quad (1)$$

where  $\xi_{\alpha}$  are the parameters that are found during MTP fitting and  $B_{\alpha}(r_i)$  are the basis functions that depend on the  $i$ -th atomic environment  $\mathbf{r}_i$  consisting of all  $j$ -th atoms that are within the distance of  $R_{\text{cut}}$  from the  $i$ -th atom, i.e.  $|r_{ij}| < R_{\text{cut}}$ .

For construction of the basis functions  $B_{\alpha}$  we introduce the moment tensor descriptors<sup>61</sup>

$$M_{\mu,\nu}(\mathbf{r}_i) = \sum_j f_{\mu}(|r_{ij}|) \underbrace{r_{ij} \otimes \dots \otimes r_{ij}}_{\nu \text{ times}}. \quad (2)$$

Here the symbol “ $\otimes$ ” denotes the outer product of the relative atomic positions  $r_{ij}$  (i.e., for  $\nu = 2$  it refers to a matrix  $r_{ij} \otimes r_{ij}$ , or, a tensor of the second rank, and for  $\nu > 2$  it refers to tensors of  $\nu$ -th rank). The first part in (2),  $f_{\mu}(|r_{ij}|)$ , is the  $\mu$ -th radial part which determines two-body interactions. We note that the radial part is the expansion over polynomials which tends to zero when the distance between atoms is close to a cut-off radius  $R_{\text{cut}}$ . The weights of this expansion is another set of MTP parameters to be fitted (see, e.g.,<sup>46</sup> for details). The second part in (2),  $r_{ij} \otimes \dots \otimes r_{ij}$ , is the angular part, it describes many-body interactions.

We then define the so-called level of the moment tensor descriptors  $\text{lev}M_{\mu,\nu} = 2 + 4\mu + \nu$ , e.g.,  $\text{lev}M_{1,0} = 6$ ,  $\text{lev}M_{2,1} =$

11,  $\text{lev}M_{0,3} = 5$ . The level of contractions, i.e., multiplication of a number of the moment tensor descriptors yielding a scalar, is defined by adding the levels, e.g.,  $\text{lev}(M_{0,1} \cdot M_{2,1}) = 11$ ,  $\text{lev}(M_{0,2} : M_{2,2}) = 16$ ,  $\text{lev}((M_{0,3}M_{1,2}) \cdot M_{0,1}) = 16$ . All such contractions of one or more moment tensor descriptors are, by definition, MTP basis functions  $B_{\alpha}$ . To define a particular functional form of MTP, we choose the maximum level,  $\text{lev}_{\text{max}}$ , and include in (1) only the basis functions with  $\text{lev}B_{\alpha} \leq \text{lev}_{\text{max}}$ .

We denote the parameters of MTP to be fitted by  $\theta$  and the MTP energy of a configuration  $\mathbf{x}$  by  $E^{\text{MTP}} = E(\theta; \mathbf{x})$ .

### B. Ab initio models

In this paper we use two models as the *ab initio* ones. The first *ab initio* (and, also, reference) model is the PES proposed in<sup>5</sup>. This model was fitted to the quantum-mechanical data (we describe the level of theory in the next paragraph) in<sup>12,13</sup> and used to predict the rate constants of the OH + HBr  $\rightarrow$  Br + H<sub>2</sub>O reaction with the quasi-classical trajectories (QCT) method. The PES has the form:

$$V(y_1, \dots, y_6) = \sum_{\substack{n_1, \dots, n_6 \\ y_2^{n_4} y_3^{n_5} y_4^{n_2} y_5^{n_3}}} C_{n_1, \dots, n_6} y_1^{n_1} y_6^{n_6} [y_2^{n_2} y_3^{n_3} y_4^{n_4} y_5^{n_5} + \quad (3)$$

where  $y_i = e^{-r_i/2a_0}$ ,  $r_i$  is an internuclear distance, namely:  $r_1 = r_{\text{HH}'}$ ,  $r_2 = r_{\text{HO}}$ ,  $r_3 = r_{\text{HBr}}$ ,  $r_4 = r_{\text{H}'\text{O}}$ ,  $r_5 = r_{\text{H}'\text{Br}}$ , and  $r_6 = r_{\text{OBr}}$ , i.e., the PES is invariant with respect to the hydrogen atom permutations. The order of the polynomials in (3) is  $n_1 + \dots + n_6 \leq 6$ , thus, we have 502 parameters. This PES is published in the open-source POTLIB code. We refer to this PES as POTLIB. We use it in our first test, namely, for comparison of the rate constants obtained with the MTP fitted to the POTLIB PES with the ones obtained with POTLIB<sup>12,13</sup> at different temperatures.

The second *ab initio* model is quantum-mechanical. It is based on the spin-unlimited method of explicitly correlated coupled clusters with allowance for double and partial allowance for triple excitations (UCCSD(T)-F12a). Quantum-mechanical calculations were carried out using the MOLPRO package. The restricted Hartree-Fock method for open shells (ROHF) was used to construct the reference functions. The calculations were performed using the cc-pVDZ-F12 orbital basis set and the following subsets: cc-pVDZ(-PP)-F12/OptRI for identity resolution, cc-pVTZ/JKFIT (for H and O), and QZVPP/JKFIT (for Br) when fitting the density of the exchange operator and the Fock operator, as well as the sets aug-cc-pVTZ/MP2FIT (for H and O) and cc-pVTZ-PP-F12/MP2FIT (for Br) for the remaining two-electron integrals. Instead of explicitly taking into account the electrons of the lowest energy levels of bromine, the effective relativistic ten-electron potential (ECP10MDF) was used. The specific choice of the method and the orbital and auxiliary basis sets were the same as in<sup>12</sup> and correspond to a high level of quantum-mechanical theory.

### C. Fitting

Assume there are  $K$  starting configurations in the training set. Each configuration  $\mathbf{x}^{(k)}$  in the training set has *ab initio* energy precalculated. We denote *ab initio* energies by  $E^{\text{a.i.}}$ . For finding the parameters  $\theta$ , i.e., MTP fitting, we minimize the loss function

$$L(\theta) = \sum_k \left( E(\theta; \mathbf{x}^{(k)}) - E^{\text{a.i.}}(\mathbf{x}^{(k)}) \right)^2 \rightarrow \min. \quad (4)$$

Starting from  $K$  initial configurations we create the training set automatically using the AL<sup>25,56</sup> algorithm during the RPMD<sup>6,10,11</sup> simulation. The AL algorithm allows us to select configurations for adding to the training set on which MTP will be trained and the RPMD method allows us calculating rate constants with high accuracy. The combination of MTP active training and RPMD methods (RPMD-AL-MTP algorithm) has already been successfully applied to the thermally activated  $\text{OH} + \text{H}_2 \rightarrow \text{H} + \text{H}_2\text{O}$ <sup>46</sup> and  $\text{CH}_4 + \text{CN} \rightarrow \text{CH}_3 + \text{HCN}$ <sup>46</sup> chemical reactions, and the barrierless  $\text{S} + \text{H}_2 \rightarrow \text{SH} + \text{H}$ <sup>49</sup> chemical reaction. However, in the mentioned studies MTP was fitted to the energies and forces calculated with the reference model PESs rather than a quantum-mechanical model. Here we go beyond the previous model calculations and also fit MTP to quantum-mechanical data. The scheme of our methodology is shown in Fig. 1.

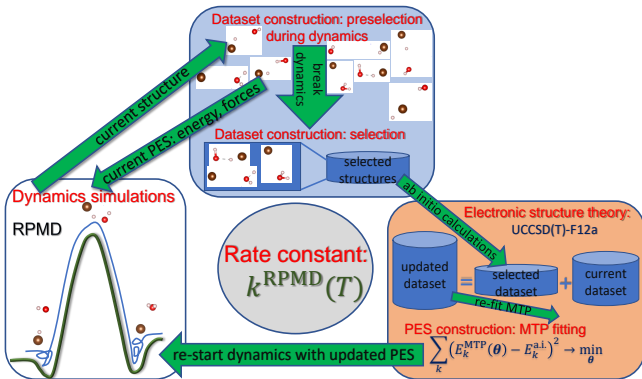


FIG. 1. Scheme of the methodology for reliable estimation of thermal rate constants based on combining the best practices for dynamic simulations (RPMD), PES construction (AL-MTP), and electronic structure calculations (UCCSD(T)-F12a). The RPMD method gives structures, we calculate their energies and forces with the current MTP and preselect some of them during dynamics. At some point we stop RPMD simulation according to the AL method, select some of the preselected structures, and conduct *ab initio* calculations for them. Finally, we update the training set (dataset) by adding the selected dataset to the current dataset, re-fit the current MTP, and re-start RPMD with the updated MTP. We continue this cycle until we obtain the final thermal rate constants.

### D. Computational details

We use the RPMDrate code<sup>66</sup> for calculating the chemical reaction  $\text{OH} + \text{HBr} \rightarrow \text{Br} + \text{H}_2\text{O}$  rate constants and the MLIP-

2 code<sup>47</sup> for the active training of MTP. POTLIB is available online<sup>1</sup>. We use the MOLPRO package for the quantum-mechanical calculations<sup>69</sup>.

In order to compare with the experimental rate coefficients, it is necessary to take OH spin-orbit coupling effects into account, which are not included in RPMD calculations. The  ${}^2\Pi_{1/2}$  excited state of OH, which is  $\Delta = 140 \text{ cm}^{-1}$  above the  ${}^2\Pi_{3/2}$  ground state can be included by considering that the ratio of transition state to reactant electronic partition functions adds a factor  $F(T)$ , as in the previous theoretical studies, in the following form:

$$F(T) = 1 + e^{-\Delta/k_B T}.$$

The resulting spin-orbit corrected rate constant is  $k_{\text{RPMD}}^{\text{corr.}}(T) = F^{-1}(T) \times k_{\text{RPMD}}(T)$ .

The QCT rate constants were calculated taking spin-orbit coupling effects into account (rigid-rotor spin-orbit (RR/SO) rate constant), neglecting them (RR/nSO rate constant), and using a detailed quantum mechanical treatment of the energy levels in a fully coupled calculation (coupled rate constant), see Ref.<sup>13</sup> for details. Here we provide the QCT coupled rate constants and deviations from them (RR/SO and RR/nSO rate constants). We note that all the three rate constants are close to each other at the considered temperatures.

We calculate the RPMD rate constants at  $T = 200, 300,$  and  $500 \text{ K}$  and consider 192, 128, and 96 ring polymer beads, respectively. In order to obtain the potential of mean force (PMF)  $W(\xi)$  along the reaction coordinate  $\xi$  we divide the interval of the coordinate  $-0.05 \leq \xi \leq 1.05$  into 111 windows of width 0.01. We determine the dynamical correction to the rate constant, namely, the recrossing factor, at the ‘‘plateau’’ time observed around 0.3 ps.

We run the calculations with the RPMD method using three PESs: POTLIB, MTP fitted to POTLIB (we denote it by MTP\_POTLIB), and MTP fitted to the quantum-mechanical calculations with the MOLPRO package (we denote it by MTP\_MOLPRO). Each MTP contains 527 parameters to optimize ( $\text{lev}_{\text{max}} = 16$ ) and the cut-off radius of  $6 \text{ \AA}$ .

## III. RESULTS

### A. Potential of mean force

The PMF profiles obtained with the POTLIB, MTP\_POTLIB, and MTP\_MOLPRO PESs at  $T = 200, 300,$  and  $500 \text{ K}$  are shown in Fig. 2. From the figure we see that the free energy has a non-trivial profile along the reaction path which includes both pre-reaction complex formation well and thermally activated free energy barrier. The interplay of these two factors depends on temperature – while at  $500 \text{ K}$  the profile is close to a standard for typical thermally activated reactions, at  $200 \text{ K}$  the complex-formation region starts to play an important role.

As it was expected, the profiles obtained with the POTLIB and MTP\_POTLIB PESs are close to each other at different temperatures. The profiles calculated with MTP\_MOLPRO

turned out to be unexpected: the difference between the minimum and maximum free energy  $W(\xi)$  is much larger for the MTP\_MOLPRO profile than the similar value for the POTLIB and MTP\_POTLIB profiles. For investigating this phenomenon, we calculated the minimum energy, energy in a saddle point, and energy barrier. The results are given in Table I.

TABLE I. Minimum energy ( $E_{\min}$ ), energy at the saddle point ( $E_{\text{saddle}}$ ), and their difference (barrier) calculated with the POTLIB PES, the MTP\_POTLIB PES, the MTP\_MOLPRO PES, and MOLPRO (0 meV corresponds to the minimum energy obtained with MOLPRO).

Model	$E_{\min}$ , meV	$E_{\text{saddle}}$ , meV	Barrier, meV
POTLIB	-1.0	103.3	104.3
MTP_POTLIB	-3.0	102.7	105.7
MTP_MOLPRO	-4.7	110.4	115.1
MOLPRO	0	112.4	112.4

Table I explains the discrepancy between the PMFs obtained with the POTLIB (or, MTP\_POTLIB) and MTP\_MOLPRO PESs in the Fig. 2. The difference between the MTP\_MOLPRO and POTLIB (or, MTP\_POTLIB) energy barriers in the Table I is of 10 meV whereas it is approximately equal to 40–50 meV in the Fig. 2 and MTP\_MOLPRO barrier is higher than the POTLIB one. The values of the energy barrier are not exactly the same because the energy barriers in the Table I do not include thermodynamic and zero point energy (ZPE) corrections, while the profiles of free energy in the Fig. 2 are calculated at non-zero temperatures, thus both the ZPE and the system entropy affect the free energy barriers. We also note that the minimum of free energy calculated at  $T = 200$  and 300 K with MTP\_MOLPRO is lower than the one obtained with POTLIB and, at the same time, the saddle point of MTP\_MOLPRO free energy is higher than the one of POTLIB. We see the same correlations for energies in Table I. Finally, the MTP\_MOLPRO and MOLPRO energy barriers are close to each other: the difference is about 3 meV. We also note that the MTP fitting error is about 3 meV per atom. Such the fitting root-mean square error is close to the root-mean square error of 1.5-2.5 meV per atom typical for the MTP of 16-th level (see, e.g., Refs.<sup>30,47,48</sup>) we use in this paper. Thus, we can conclude that MTP was accurately fitted to the quantum-mechanical data.

**B. Rescoring factor**

The profiles of the rescoring factor obtained with different PESs at  $T = 200, 300,$  and  $500$  K are demonstrated in Fig. 3. As in the case of PMF profiles, the rescoring factors obtained with the POTLIB and MTP\_POTLIB PESs are close to each other. The MTP\_MOLPRO rescoring factor at  $T = 300$  K is slightly larger than the ones obtained with the PESs on the basis of POTLIB, however, the relative difference is not as large as for the free energy. Finally, all the three models give very close rescoring factors at  $T = 200$  K and  $T = 500$  K.

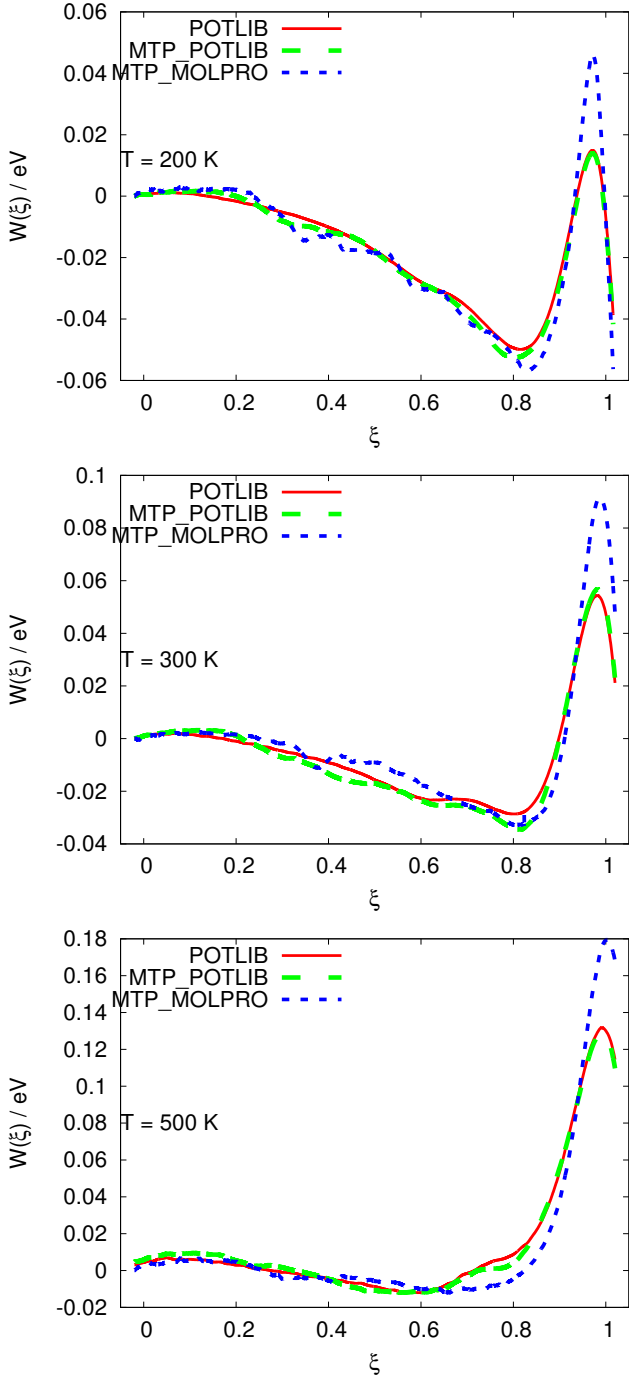


FIG. 2. Potentials of mean force obtained with different PESs at  $T = 200, 300,$  and  $500$  K.

**C. Theoretical and experimental thermal rate constants**

The theoretical and experimental thermal rate constants of the  $\text{OH} + \text{HBr} \rightarrow \text{Br} + \text{H}_2\text{O}$  reaction are given in Table II. The theoretical rate constants were calculated with the RPMD method using three PESs: POTLIB, MTP\_POTLIB, and MTP\_MOLPRO. We denote them by  $k_{\text{RPMD}}$ . We compare the calculated  $k_{\text{RPMD}}$  constants with the theoretical  $k_{\text{QCT}}$

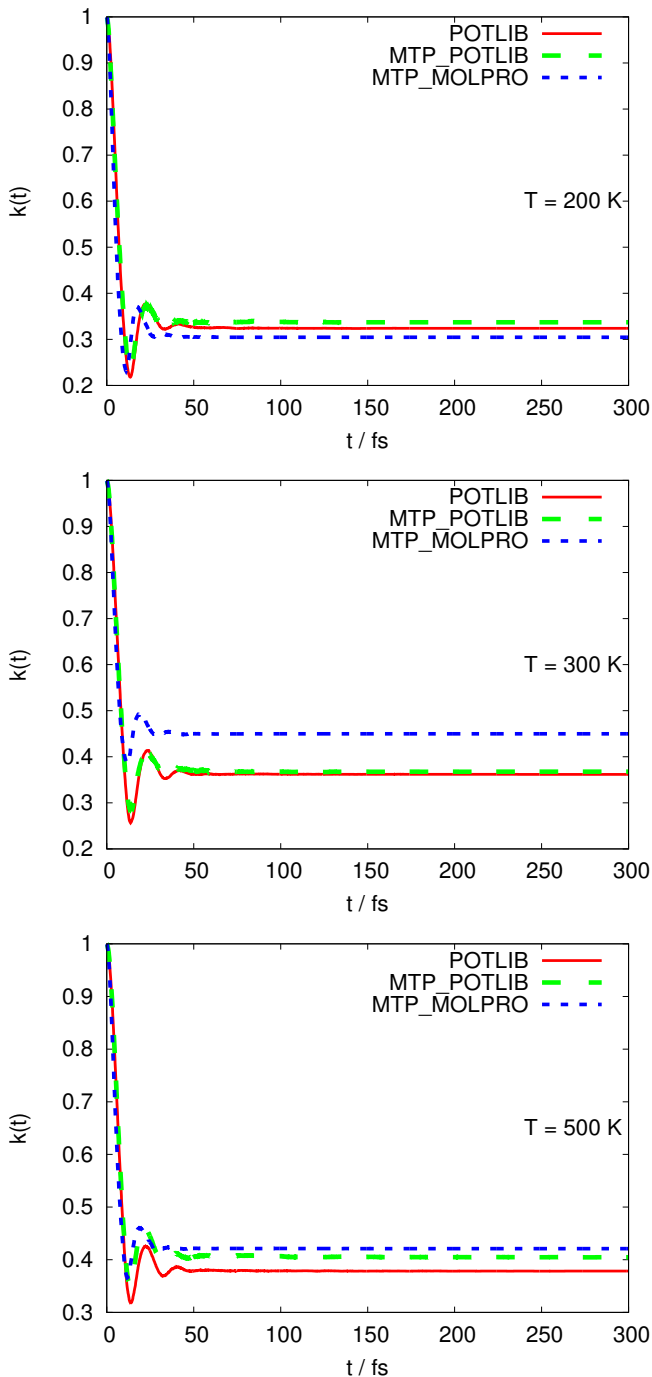


FIG. 3. Recrossing factors obtained with different PESs at  $T = 200$ , 300, and 500 K.

constants obtained with the QCT method using the POTLIB PES and with the experimental  $k_{\text{exp}}$  constants. The  $k_{\text{QCT}}$  and  $k_{\text{exp}}$  constants were taken from Refs.<sup>3,13,32–34,45,59,60,62,67</sup>.

Several important conclusions can be drawn from Table II. Firstly, the  $k_{\text{QCT}}$  and  $k_{\text{RPMD}}$  rate constants calculated with the POTLIB PES are of the same order of magnitude, but there are differences in the absolute values. The rate constants are almost the same at  $T = 500$  K, the difference between them is

TABLE II. Comparison of the thermal rate constants, obtained theoretically (with the RPMD and QCT<sup>13</sup> methods) and experimentally<sup>3,32–34,45,59,60,62,67</sup>. The values of the constants are given in  $10^{-11} \text{ cm}^3 \cdot (\text{molecule})^{-1} \text{ s}^{-1}$ .

$T$ , K	$k_{\text{QCT}}$ POTLIB	$k_{\text{RPMD}}$ POTLIB	$k_{\text{RPMD}}$ MTP_POTLIB	$k_{\text{RPMD}}$ MTP_MOLPRO	$k_{\text{exp}}$
200	$2.5 \pm 0.5$	8.3	13	1.41	$1.35 \pm 0.65$
300	$1.75 \pm 0.25$	3.2	3.0	0.94	$1.0 \pm 0.2$
500	$1.4 \pm 0.2$	1.7	2.1	0.63	$1.0 \pm 0.2$

at around 20% which corresponds to the accuracy of the RPMDrate methodology<sup>63,66</sup>. The  $k_{\text{RPMD}}$  rate constant is greater than the  $k_{\text{QCT}}$  rate constant by factors of 1.8 and 3.3 at  $T = 300$  K and  $T = 500$  K, respectively. However, the trend of rate constant decreasing with temperature increasing was reproduced by the RPMD method.

Secondly, we compared the  $k_{\text{RPMD}}$  thermal rate constants obtained with the POTLIB and MTP\_POTLIB PESs obtained using RPMD-AL-MTP algorithm. The rate constants at  $T = 300$  K and  $T = 500$  K are in a good agreement to each other, the accuracy of their calculation is close to the accuracy of the RPMD method. For  $T = 200$  K, the error in determining the rate constant was 50%. A possible reason for this difference is a rather small barrier in the free energy profile (about 70 meV, see Fig. 2) and, therefore, even the small difference in the profiles can significantly affect the resulting rate constant. One of the solutions to this problem could be to increase the number of MTP parameters, however, the exact reproduction of the results of the POTLIB PES using MTP was not the main aim of this paper and, thus, we did not increase the number of MTP parameters. As for the POTLIB potential, the trend of rate constant decreasing with temperature increasing temperature was reproduced by the RPMD-AL-MTP method.

Finally, we compared all the theoretical and experimental thermal rate constants. The closest to the experimental rate constants were the ones obtained using the MTP\_MOLPRO: the agreement between MTP\_MOLPRO and the experimental constants was almost perfect at  $T = 200$  and 300 K, while the constant obtained at  $T = 500$  K with the MTP\_MOLPRO is closer to the experimental constants than all the other theoretical constants. We note that all the data in the paper<sup>13</sup> are published up to a temperature of 450 K. However, the rate constants change insignificantly at the temperatures higher than 400 K and the comparison at  $T = 500$  K makes sense. We also emphasize that we did not consider the temperatures lower than 200 K as the experimental rate constants represented in the paper<sup>13</sup> under this temperature have large standard deviation.

The above results demonstrate that the chemical reaction rate constants obtained with RPMD-AL-MTP method using MTP\_MOLPRO are closer to the experimental ones than the previous theoretical constants. Thus, the RPMD-AL-MTP method, when using data from quantum-mechanical calculations for MTP training, is more accurate than the QCT method with the POTLIB PES trained to the data obtained at the same

level of quantum-mechanical theory, at least for the title reaction for a wide temperature range.

#### IV. CONCLUSIONS

In summary, in this paper we calculated thermal rate constants of the thermally activated  $\text{OH} + \text{HBr} \rightarrow \text{Br} + \text{H}_2\text{O}$  chemical reaction which is of great importance for stratospheric chemistry as it is the major process by which atomic bromine, an active ozone depletion catalyst, is regenerated from the relatively stable hydrogen bromide. We used the combination of Active Learning of Moment Tensor Potential (AL-MTP) fitted to the data obtained with the spin-unlimited method of explicitly correlated coupled clusters with allowance for double and partial allowance for triple excitations (UCCSD(T)-F12a) and Ring Polymer Molecular Dynamics (RPMD). The rate constants obtained with the RPMD-AL-MTP method at  $T = 200, 300,$  and  $500$  K were compared with the ones obtained previously with the method of quasiclassical trajectories (QCT) using the POTLIB PES and with the experimental ones published earlier. Both the MTP and POTLIB potentials were parameterized to the data obtained at the same high level of quantum-mechanical theory. The rate constants calculated with the MTP fitted to the quantum-mechanical data are in the best correspondence with the experimental ones than the other theoretical rate constants, including the QCT ones, at all the three considered temperatures. Thus, we have demonstrated, that the proposed methodology based on combining best practices for electronic structure calculations (UCCSD(T)-F12a), PES construction (AL-MTP) and dynamic simulations (RPMD) makes theoretical estimation of thermal rate constants reliable and can be with certainty extended to more complex and important gas-phase chemical reactions in future.

#### CONFLICTS OF INTEREST

There are no conflicts to declare.

#### ACKNOWLEDGEMENTS

This work was supported by the Russian Foundation for Basic Research (grant number 20-03-00833).

<sup>1</sup><https://comp.chem.umn.edu/potlib/showPotential.cgi?id=H2OBr>, 2014.

<sup>2</sup>Joshua W Allen, William H Green, Yongle Li, Hua Guo, and Yury V Suleimanov. Communication: Full dimensional quantum rate coefficients and kinetic isotope effects from ring polymer molecular dynamics for a seven-atom reaction  $\text{OH} + \text{CH}_4 \rightarrow \text{CH}_3 + \text{H}_2\text{O}$ , 2013.

<sup>3</sup>Dean B Atkinson, Veronica I Jaramillo, and Mark A Smith. Low-temperature kinetic behavior of the bimolecular reaction  $\text{oh} + \text{hbr}$  (76–242 k). *The Journal of Physical Chemistry A*, 101(18):3356–3359, 1997.

<sup>4</sup>Somnath Bhowmick, Duncan Bossion, Yohann Scribano, and Yury V Suleimanov. The low temperature  $\text{D}^+ + \text{H}_2 \rightarrow \text{HD} + \text{H}^+$  reaction rate coefficient: A ring polymer molecular dynamics and quasi-classical trajectory study. *Physical Chemistry Chemical Physics*, 20(41):26752–26763, 2018.

<sup>5</sup>Bastiaan J Braams and Joel M Bowman. Permutationally invariant potential energy surfaces in high dimensionality. *International Reviews in Physical Chemistry*, 28(4):577–606, 2009.

<sup>6</sup>Bastiaan J Braams and David E Manolopoulos. On the short-time limit of ring polymer molecular dynamics. *J. Chem. Phys.*, 125(12):124105, 2006.

<sup>7</sup>JF Castillo and YV Suleimanov. A ring polymer molecular dynamics study of the  $\text{OH} + \text{H}_2(\text{D}_2)$  reaction. *Phys. Chem. Chem. Phys.*, 19(43):29170–29176, 2017.

<sup>8</sup>DR Clark, RF Simmons, and DA Smith. Inhibition of the second limit of the hydrogen + oxygen reaction by hydrogen bromide. *Transactions of the Faraday Society*, 66:1423–1435, 1970.

<sup>9</sup>Michael A Collins. Molecular potential-energy surfaces for chemical reaction dynamics. *Theoretical Chemistry Accounts*, 108(6):313–324, 2002.

<sup>10</sup>Ian R Craig and David E Manolopoulos. Quantum statistics and classical mechanics: Real time correlation functions from ring polymer molecular dynamics. *J. Chem. Phys.*, 121(8):3368–3373, 2004.

<sup>11</sup>Ian R Craig and David E Manolopoulos. A refined ring polymer molecular dynamics theory of chemical reaction rates. *J. Chem. Phys.*, 123(3):034102, 2005.

<sup>12</sup>Antonio GS de Oliveira-Filho, Fernando R Ornellas, and Joel M Bowman. Energy disposal and thermal rate constants for the  $\text{oh} + \text{hbr}$  and  $\text{oh} + \text{dbr}$  reactions: quasiclassical trajectory calculations on an accurate potential energy surface. *The Journal of Physical Chemistry A*, 118(51):12080–12088, 2014.

<sup>13</sup>Antonio GS de Oliveira-Filho, Fernando R Ornellas, and Joel M Bowman. Quasiclassical trajectory calculations of the rate constant of the  $\text{oh} + \text{hbr} \rightarrow \text{br} + \text{h}_2\text{o}$  reaction using a full-dimensional ab initio potential energy surface over the temperature range 5 to 500 k. *The journal of physical chemistry letters*, 5(4):706–712, 2014.

<sup>14</sup>Pablo del Mazo-Sevillano, Alfredo Aguado, Elena Jiménez, Yury V Suleimanov, and Octavio Roncero. Quantum roaming in the complex-forming mechanism of the reactions of  $\text{oh}$  with formaldehyde and methanol at low temperature and zero pressure: A ring polymer molecular dynamics approach. *The journal of physical chemistry letters*, 10(8):1900–1907, 2019.

<sup>15</sup>Ronald J Duchovic, Yuri L Volobuev, Gillian C Lynch, Donald G Truhlar, Thomas C Allison, Albert F Wagner, Bruce C Garrett, and Jose C Corchado. Potlib 2001: A potential energy surface library for chemical systems. *Computer physics communications*, 144(2):169–187, 2002.

<sup>16</sup>Joaquin Espinosa-Garcia, Moises Garcia-Chamorro, Jose Carlos Corchado, Somnath Bhowmick, and Yury Suleimanov. Vtst and rpmd kinetics study of the nine-body  $\text{X} + \text{C}_2\text{H}_6$  ( $\text{X} = \text{H}, \text{Cl}, \text{F}$ ) reactions based on analytical potential energy surfaces. *Physical Chemistry Chemical Physics*, 2020.

<sup>17</sup>Joaquin Espinosa-Garcia, Cipriano Rangel, and Yury V Suleimanov. Kinetics study of the  $\text{CN} + \text{CH}_4$  hydrogen abstraction reaction based on a new ab initio analytical full-dimensional potential energy surface. *Phys. Chem. Chem. Phys.*, 19(29):19341–19351, 2017.

<sup>18</sup>Reinhard Farwig. Rate of convergence of shepard’s global interpolation formula. *Mathematics of Computation*, 46(174):577–590, 1986.

<sup>19</sup>Axel Forslund, Xi Zhang, Blazej Grabowski, Alexander V Shapeev, and Andrei V Ruban. Ab initio simulations of the surface free energy of tin (001). *Physical Review B*, 103(19):195428, 2021.

<sup>20</sup>Eloisa Gonzalez-Lavado, Jose C Corchado, Yury V Suleimanov, William H Green, and Joaquin Espinosa-Garcia. Theoretical kinetics study of the  $\text{O}(^3\text{P}) + \text{CH}_4/\text{CD}_4$  hydrogen abstraction reaction: the role of anharmonicity, recrossing effects, and quantum mechanical tunneling. *The Journal of Physical Chemistry A*, 118(18):3243–3252, 2014.

<sup>21</sup>Blazej Grabowski, Yuji Ikeda, Prashanth Srinivasan, Fritz Körmann, Christoph Freysoldt, Andrew Ian Duff, Alexander Shapeev, and Jörg Neugebauer. Ab initio vibrational free energies including anharmonicity for multicomponent alloys. *npj Computational Materials*, 5(1):1–6, 2019.

<sup>22</sup>K. Gubaev, E. Podryabinkin, Gus L.W. Hart, and A. Shapeev. Accelerating high-throughput search for new alloys with active learning of interatomic potentials. Work in progress.

<sup>23</sup>Konstantin Gubaev, Yuji Ikeda, Ferenc Tasnádi, Jörg Neugebauer, Alexander V Shapeev, Blazej Grabowski, and Fritz Körmann. Finite-temperature interplay of structural stability, chemical complexity, and elastic properties of bcc multicomponent alloys from ab initio trained machine-learning potentials. *Physical Review Materials*, 5(7):073801, 2021.

- <sup>24</sup>Konstantin Gubaev, Evgeny V Podryabinkin, Gus LW Hart, and Alexander V Shapeev. Accelerating high-throughput searches for new alloys with active learning of interatomic potentials. *Computational Materials Science*, 156(24):148–156, 2019.
- <sup>25</sup>Konstantin Gubaev, Evgeny V Podryabinkin, and Alexander V Shapeev. Machine learning of molecular properties: Locality and active learning. *J. Chem. Phys.*, 148(24):241727, 2018.
- <sup>26</sup>Kevin M Hickson, Somnath Bhowmick, Yury V Suleimanov, João Brandão, and Daniela V Coelho. Experimental and theoretical studies of the gas-phase reactions of  $\text{o}(1\text{d})$  with  $\text{h}_2\text{o}$  and  $\text{d}_2\text{o}$  at low temperature. *Physical Chemistry Chemical Physics*, 23(45):25797–25806, 2021.
- <sup>27</sup>Kevin M. Hickson, Jean-Christophe Loison, Hua Guo, and Yury V. Suleimanov. Ring-polymer molecular dynamics for the prediction of low-temperature rates: An investigation of the  $\text{c}(1\text{d}) + \text{h}_2$  reaction. *J. Phys. Chem. Lett.*, 6(21):4194–4199, 2015.
- <sup>28</sup>Kevin M Hickson and Yury V Suleimanov. An experimental and theoretical investigation of the  $\text{C}(1\text{D}) + \text{D}_2$  reaction. *Physical Chemistry Chemical Physics*, 19(1):480–486, 2017.
- <sup>29</sup>Kevin M Hickson and Yury V Suleimanov. Low-temperature experimental and theoretical rate constants for the  $\text{O}(1\text{D}) + \text{H}_2$  reaction. *The Journal of Physical Chemistry A*, 121(9):1916–1923, 2017.
- <sup>30</sup>Max Hodapp and Alexander Shapeev. Machine-learning potentials enable predictive and tractable high-throughput screening of random alloys. *Physical Review Materials*, 5(11):113802, 2021.
- <sup>31</sup>Mehdi Jafary-Zadeh, Khoong Hong Khoo, Robert Laskowski, Paulo S Branicio, and Alexander V Shapeev. Applying a machine learning interatomic potential to unravel the effects of local lattice distortion on the elastic properties of multi-principal element alloys. *Journal of Alloys and Compounds*, 803:1054–1062, 2019.
- <sup>32</sup>Veronica I Jaramillo, Samuel Gougeon, Sébastien D Le Picard, André Canosa, Mark A Smith, and Bertrand R Rowe. A consensus view of the temperature dependence of the gas phase reaction:  $\text{Oh} + \text{hbr} \rightarrow \text{h}_2\text{o} + \text{br}$ . *International journal of chemical kinetics*, 34(6):339–344, 2002.
- <sup>33</sup>Veronica I Jaramillo and Mark A Smith. Temperature-dependent kinetic isotope effects in the gas-phase reaction:  $\text{Oh} + \text{hbr}$ . *The Journal of Physical Chemistry A*, 105(24):5854–5859, 2001.
- <sup>34</sup>JL Jourdain, G Le Bras, and J Combourieu. Epr determination of absolute rate constants for the reactions of  $\text{h}$  and  $\text{oh}$  radicals with hydrogen bromide. *Chemical Physics Letters*, 78(3):483–487, 1981.
- <sup>35</sup>Pavel Yu Korotaev, Ivan I Novoselov, Aleksey V Yanilkin, and Alexander V Shapeev. Accessing thermal conductivity of complex compounds by machine learning interatomic potentials. *Physical Review B*, 100(14):144308, 2019.
- <sup>36</sup>Sunil S Kumar, Florian Grussie, Yury V Suleimanov, Hua Guo, and Holger Kreckel. Low temperature rates for key steps of interstellar gas-phase water formation. *Science advances*, 4(6):eaar3417, 2018.
- <sup>37</sup>V Ladygin, I Beniya, E Makarov, and A Shapeev. Bayesian learning of thermodynamic integration and numerical convergence for accurate phase diagrams. *Physical Review B*, 104(10):104102, 2021.
- <sup>38</sup>Vladimir V Ladygin, Pavel Yu Korotaev, Aleksey V Yanilkin, and Alexander V Shapeev. Lattice dynamics simulation using machine learning interatomic potentials. *Computational Materials Science*, 172:109333, 2020.
- <sup>39</sup>Yongle Li, Yury V Suleimanov, William H Green, and Hua Guo. Quantum rate coefficients and kinetic isotope effect for the reaction  $\text{Cl} + \text{CH}_4 \rightarrow \text{HCl} + \text{CH}_3$  from ring polymer molecular dynamics. *The Journal of Physical Chemistry A*, 118(11):1989–1996, 2014.
- <sup>40</sup>M Menendez, PG Jambrina, A Zanchet, E Verdasco, YV Suleimanov, and FJ Aoiz. New stress test for ring polymer molecular dynamics: Rate coefficients of the  $\text{o}(3\text{p}) + \text{hcl}$  reaction and comparison with quantum mechanical and quasiclassical trajectory results. *The Journal of Physical Chemistry A*, 123(37):7920–7931, 2019.
- <sup>41</sup>Bohayra Mortazavi, Brahmanandam Javvaji, Fazel Shojaei, Timon Rabczuk, Alexander V Shapeev, and Xiaoying Zhuang. Exceptional piezoelectricity, high thermal conductivity and stiffness and promising photocatalysis in two-dimensional  $\text{mosi}_2\text{zn}_4$  family confirmed by first-principles. *Nano Energy*, 82:105716, 2021.
- <sup>42</sup>Bohayra Mortazavi, Ivan S Novikov, Evgeny V Podryabinkin, Stephan Roche, Timon Rabczuk, Alexander V Shapeev, and Xiaoying Zhuang. Exploring phononic properties of two-dimensional materials using machine learning interatomic potentials. *Applied Materials Today*, 20:100685, 2020.
- <sup>43</sup>Bohayra Mortazavi, Evgeny V Podryabinkin, Ivan S Novikov, Stephan Roche, Timon Rabczuk, Xiaoying Zhuang, and Alexander V Shapeev. Efficient machine-learning based interatomic potentials for exploring thermal conductivity in two-dimensional materials. *Journal of Physics: Materials*, 2020.
- <sup>44</sup>Bohayra Mortazavi, Mohammad Silani, Evgeny V Podryabinkin, Timon Rabczuk, Xiaoying Zhuang, and Alexander V Shapeev. First-principles multiscale modeling of mechanical properties in graphene/borophene heterostructures empowered by machine-learning interatomic potentials. *Advanced Materials*, 33(35):2102807, 2021.
- <sup>45</sup>Christopher Mullen and Mark A Smith. Temperature dependence and kinetic isotope effects for the  $\text{oh} + \text{hbr}$  reaction and  $\text{h/d}$  isotopic variants at low temperatures (53–135 k) measured using a pulsed supersonic laval nozzle flow reactor. *The Journal of Physical Chemistry A*, 109(17):3893–3902, 2005.
- <sup>46</sup>I. S. Novikov, Y. V. Suleimanov, and A. V. Shapeev. Automated calculation of thermal rate coefficients using ring polymer molecular dynamics and machine-learning interatomic potentials with active learning. *Phys. Chem. Chem. Phys.*, 20:29503–29512, 2018.
- <sup>47</sup>Ivan S Novikov, Konstantin Gubaev, Evgeny V Podryabinkin, and Alexander V Shapeev. The mlip package: moment tensor potentials with mpi and active learning. *Machine Learning: Science and Technology*, 2(2):025002, 2020.
- <sup>48</sup>Ivan S Novikov and Alexander V Shapeev. Improving accuracy of interatomic potentials: more physics or more data? a case study of silica. *Materials Today Communications*, 18:74–80, 2019.
- <sup>49</sup>Ivan S Novikov, Alexander V Shapeev, and Yury V Suleimanov. Ring polymer molecular dynamics and active learning of moment tensor potential for gas-phase barrierless reactions: Application to  $\text{s} + \text{h}_2$ . *The Journal of chemical physics*, 151(22):224105, 2019.
- <sup>50</sup>Ivan I Novoselov, Aleksey V Yanilkin, Alexander V Shapeev, and Evgeny V Podryabinkin. Moment tensor potentials as a promising tool to study diffusion processes. *Computational Materials Science*, 165(15):46–56, 2019.
- <sup>51</sup>Dianailys Nuñez-Reyes, Kevin M Hickson, Pascal Larrégaray, Laurent Bonnet, Tomás González-Lezana, Somnath Bhowmick, and Yury V Suleimanov. Experimental and theoretical study of the  $\text{o}(1\text{d}) + \text{hd}$  reaction. *The Journal of Physical Chemistry A*, 123(38):8089–8098, 2019.
- <sup>52</sup>Dianailys Nuñez-Reyes, Kevin M Hickson, Pascal Larrégaray, Laurent Bonnet, Tomás González-Lezana, and Yury V Suleimanov. A combined theoretical and experimental investigation of the kinetics and dynamics of the  $\text{o}(1\text{d}) + \text{d}_2$  reaction at low temperature. *Physical Chemistry Chemical Physics*, 20(6):4404–4414, 2018.
- <sup>53</sup>Ricardo Pérez de Tudela, F. J. Aoiz, Yury V. Suleimanov, and David E. Manolopoulos. Chemical reaction rates from ring polymer molecular dynamics: Zero point energy conservation in  $\text{mu} + \text{h}_2 \rightarrow \text{muh} + \text{h}$ . *J. Phys. Chem. Lett.*, 3(4):493–497, 2012.
- <sup>54</sup>Ricardo Pérez de Tudela, Yury V. Suleimanov, Jeremy O. Richardson, Vicente Sáez Rábanos, William H. Green, and F. J. Aoiz. Stress test for quantum dynamics approximations: Deep tunneling in the muonium exchange reaction  $\text{d} + \text{hmu} \rightarrow \text{dmu} + \text{h}$ . *J. Phys. Chem. Lett.*, 5(23):4219–4224, 2014.
- <sup>55</sup>Evgeny V Podryabinkin, Alexander G Kvashnin, Milad Asgarpour, Igor I Maslenikov, Danila A Ovsyannikov, Pavel B Sorokin, Mikhail Yu Popov, and Alexander V Shapeev. Nanohardness from first principles with active learning on atomic environments. *Journal of Chemical Theory and Computation*, 2022.
- <sup>56</sup>Evgeny V Podryabinkin and Alexander V Shapeev. Active learning of linearly parametrized interatomic potentials. *Comput. Mater. Sci.*, 140:171–180, 2017.
- <sup>57</sup>Evgeny V Podryabinkin, Evgeny V Tikhonov, Alexander V Shapeev, and Artem R Oganov. Accelerating crystal structure prediction by machine-learning interatomic potentials with active learning. *Physical Review B*, 99(6):064114, 2019.
- <sup>58</sup>Sergio Rampino and Yury V Suleimanov. Thermal rate coefficients for the astrochemical process  $\text{C} + \text{CH}^+ \rightarrow \text{C}_2^+ + \text{H}$  by ring polymer molecular dynamics. *The Journal of Physical Chemistry A*, 120(50):9887–9893, 2016.
- <sup>59</sup>AR Ravishankara, PH Wine, and AO Langford. Absolute rate constant for the reaction  $\text{oh} + \text{hbr} \rightarrow \text{h}_2\text{o} + \text{br}$ . *Chemical Physics Letters*, 63(3):479–484, 1979.

- <sup>60</sup>AR Ravishankara, PH Wine, and JR Wells. The  $\text{oh} + \text{hbr}$  reaction revisited. *The Journal of chemical physics*, 83(1):447–448, 1985.
- <sup>61</sup>A.V. Shapeev. Moment tensor potentials: a class of systematically improvable interatomic potentials. *Multiscale Model. Simul.*, 14(3):1153–1173, 2016.
- <sup>62</sup>IR Sims, IWM Smith, DC Clary, P Bocherel, and BR Rowe. Ultra-low temperature kinetics of neutral–neutral reactions: New experimental and theoretical results for  $\text{oh} + \text{hbr}$  between 295 and 23 k. *The Journal of chemical physics*, 101(2):1748–1751, 1994.
- <sup>63</sup>Yury V. Suleimanov, F. Javier Aoiz, and Hua Guo. Chemical reaction rate coefficients from ring polymer molecular dynamics: Theory and practical applications. *The Journal of Physical Chemistry A*, 120(43):8488–8502, 2016. PMID: 27627634.
- <sup>64</sup>Yury V Suleimanov, Rosana Collepardo-Guevara, and David E Manolopoulos. Bimolecular reaction rates from ring polymer molecular dynamics: Application to  $\text{H} + \text{CH}_4 \rightarrow \text{H}_2 + \text{CH}_3$ . *J. Chem. Phys.*, 134(4):044131, 2011.
- <sup>65</sup>Yury V Suleimanov, Wendi J Kong, Hua Guo, and William H Green. Ring-polymer molecular dynamics: Rate coefficient calculations for energetically symmetric (near thermoneutral) insertion reactions  $(\text{X} + \text{H}_2) \rightarrow \text{HX} + \text{H}$  ( $\text{X} = \text{C}^{(1\text{D})}, \text{S}^{(1\text{D})}$ ). *The Journal of chemical physics*, 141(24):244103, 2014.
- <sup>66</sup>Yu.V. Suleimanov, J.W. Allen, and W.H. Green. Rpmbrate: Bimolecular chemical reaction rates from ring polymer molecular dynamics. *Comp. Phys. Comm.*, 184(3):833–840, 2013.
- <sup>67</sup>GA Takacs and GP Glass. Reactions of hydrogen atoms and hydroxyl radicals with hydrogen bromide. *The Journal of Physical Chemistry*, 77(8):1060–1064, 1973.
- <sup>68</sup>Ferenc Tasnádi, Florian Bock, Johan Tidholm, Alexander V Shapeev, and Igor A Abrikosov. Efficient prediction of elastic properties of  $\text{TiO}_5$  and  $\text{Sn}$  at elevated temperature using machine learning interatomic potential. *Thin Solid Films*, 737:138927, 2021.
- <sup>69</sup>Hans-Joachim Werner, Peter J Knowles, Gerald Knizia, Frederick R Manby, and Martin Schütz. Molpro: a general-purpose quantum chemistry program package. *Wiley Interdisciplinary Reviews: Computational Molecular Science*, 2(2):242–253, 2012.
- <sup>70</sup>YL Yung, JP Pinto, RT Watson, and SP Sander. Atmospheric bromine and ozone perturbations in the lower stratosphere. *Journal of Atmospheric Sciences*, 37(2):339–353, 1980.